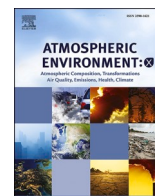


Contents lists available at [ScienceDirect](https://www.sciencedirect.com)

Atmospheric Environment: X

journal homepage: <http://www.journals.elsevier.com/atmospheric-environment-x>

Seasonality of ship emission related atmospheric pollution over coastal and open waters of the North Sea

László Bencs^{a,b,*}, Benjamin Horemans^a, Anna Jolanta Buczyńska^{a,c}, Felix Deutsch^d,
Bart Degraeuwe^d, Martine Van Poppel^d, René Van Grieken^a

^a Department of Chemistry, University of Antwerp (UA), Groenenborgerlaan 171, B-2020, Antwerp, Belgium

^b Institute for Solid State Physics and Optics, Wigner Research Centre for Physics, Hungarian Academy of Sciences, P.O. Box 49, H-1525, Budapest, Hungary

^c Department of Geology and Environmental Geosciences, Northern Illinois University, DeKalb, IL, 60115-2828, USA

^d Flemish Institute for Technological Research (VITO), Boeretang 200, B-2400, Mol, Belgium

ARTICLE INFO

Keywords:

Mobile emission sources
Ocean-going ship emission
Exhaust plume
Oceanic air pollutants
Seasonality
Chemical mass closure

ABSTRACT

The seasonal changes of a large set of atmospheric pollutants (i.e., gases, water-soluble aerosols, metallic/elemental components and black carbon (BC) content) have been studied over the southern bight of the North Sea (the Belgian Continental Shelf) and the English Channel during several marine sampling campaigns, carried out in 2010–2011. A coastal research station at De Haan, Belgium was concurrently used as a background air monitoring site. Size-segregated aerosols (PM₁, PM_{2.5-1}, PM_{10-2.5}) were analyzed for particulate mass, elemental content and water-soluble (ionic) compounds, while the equivalent BC content in PM₁₀ was monitored with an Aethalometer. The results clearly demonstrated that the aerosols originating from ship exhaust emissions contributed mostly to fine fraction (PM₁), and to a lesser extent to medium-sized fraction (PM_{2.5-1}), whereas components of sea spray and of mineral/soil origin were dominating in the medium-size and coarse aerosol fractions. Looking at seasonal differences, more ship emission related components occurred in the fine and medium-sized PM during winter. Mineral aerosol components were more apparent in coarse PM and especially during the cold season, increased levels were noted. Similarly, higher concentrations of marine fine PM were found during winter, likely due to more extensive ship emissions and/or calm weather conditions. Gaseous pollutants (e.g., HNO₂, HNO₃, HCl, SO₂, NH₃) originating from exhaust fumes of ocean-going ships mostly reached the maximum levels in the cold season as well, thus supporting the more intense formation of secondary aerosols. The seasonal trends of total (inorganic) ionic species sampled on the open sea and at the coastal station were usually similar to those of the corresponding PM masses, peaking in the cold season. Sea salt bound fine sulfate and nitrate peaked in spring or the cold season for marine areas, whereas for the coastal site they clearly reached the maximum in the cold season. Ammonium-bound nitrates and sulfates in each PM fraction reached their peak air levels in the cold season over marine sites. Similar seasonal trends could be observed for the coastal station. The general tendency of aerosol distribution over the study areas was independent of the sampling site: the higher the aerosol mass on the open sea with ship traffic, the higher the suspended particulate mass sampled at the coast.

Introduction

Exhaust plumes from large-sized sea-going cargo and passenger ships have been reported to contribute considerably to poor air quality (Cooper et al., 1996; Cooper, 2001, 2003; Davis et al., 2001; Eyring et al., 2010; De Meyer et al., 2008; Agrawal et al., 2008; Dalsøren et al., 2009; Alföldy et al., 2013; Tao et al., 2017; Chu-Van et al., 2018). This type of anthropogenic air pollution can heavily affect the nutrient

concentration and contamination burden of various marine regions (De Meyer et al., 2008; Bencs et al., 2017), as well as coastal (Poplawski et al., 2011; Tao et al., 2017; Bencs et al., 2017; Alver et al., 2018; Liu et al., 2018; Wang et al., 2018; Xu et al., 2018) and continental areas (Querol et al., 2007; de la Rosa et al., 2010; Pandolfi et al., 2011; Blasco et al., 2014; Tao et al., 2017; Li et al., 2018; Liu et al., 2018; Xu et al., 2018; Murena et al., 2018). Other important studies on ship emissions investigated various physico-chemical properties of aerosols released by

* Corresponding author. Department of Chemistry, University of Antwerp (UA), Groenenborgerlaan 171, B-2020, Antwerp, Belgium.

E-mail address: bencs.laszlo@wigner.mta.hu (L. Bencs).

<https://doi.org/10.1016/j.aeoa.2020.100077>

Received 31 August 2019; Received in revised form 3 May 2020; Accepted 7 May 2020

Available online 14 May 2020

2590-1621/© 2020 The Authors.

Published by Elsevier Ltd.

This is an open access article under the CC BY-NC-ND license

(<http://creativecommons.org/licenses/by-nc-nd/4.0/>).

international shipping operations (Chen et al., 2005; Lack et al., 2009; Moldanová et al., 2009; Popovicheva et al., 2012). These research groups were focusing on the exact chemical composition, distribution, morphology and optical properties of aerosols.

According to model studies, ship emission released pollution affects the air-quality of various urban and natural preservation areas (Mölders et al., 2010). For instance, it contributes 30–40% and 10% of the total PM_{2.5} and PM₁₀ concentrations, respectively, and causes an increase in concentrations of NO_x (90%), O₃ (<5%), HNO₃ (+100 pptv), and PAN (>18 pptv) along sea lanes and adjacent coastal sites. Besides, the emission products of ship traffic could reduce the visibility in these areas as seriously as by 30%. Adverse human health effects can be considerably higher at populated areas located near marine environments with dense ship traffic (Corbett et al., 2007). Consequently, the monitoring of these pollutants over marine and coastal areas is of paramount importance in the identification and characterization of ship emissions related pollution, as well as in assessment of their exact risks to health of the population living in nearby regions.

Annual ship emissions from the Belgian North Sea with a total water surface of 3600 km², were estimated for SO₂, NO_x and CO₂ by taking into account national and international ship traffic density, power and fuel usage of the ships/boats involved in the traffic on these areas (De Meyer et al., 2008). These ship emission estimates are based on bottom-up, activity based methodology, covering more than 90% of the ship activity over the region, complemented with a top-down fuel consumption methodology for the remaining activities. Compared to the Belgian National Inventory Data, the obtained emissions of SO₂ and NO_x correspond to 30% and 22% of the total national emission, thus each represents a significant contribution to anthropogenically induced pollution burden to the environment (De Meyer et al., 2008). Recently, Åström et al. (2018) analyzed the costs and benefits of a nitrogen emission control area (NECA) in the Baltic Sea and the North Sea for 2030. They assessed the emission control costs for shipping, using various models (e.g., GAINS, Alpha-RiskPoll) for emission dispersion calculations and human health impacts. The authors concluded that the NECAs for the Baltic Sea and the North Sea can be justified using cost and benefit analysis under all, but extreme assumptions.

According to the ship emissions related literature, there is a certain gap of knowledge regarding the seasonality of gaseous pollutants and size-segregated aerosol, as well as characterization of their fate (sources/transport/transformation/deposition) over North Sea waters. Especially the role of pollutants released from large cargo/ferry boats taking part in the national and international ship-traffic has not yet been characterized in terms of seasonal trends and compositions. In addition, ship-released atmospheric nutrients and toxic substances deposited to the marine environment can be accumulated and amplified in the food chain, and may also contribute to coastal eutrophication too. Therefore, their influence on marine ecosystems needs to be systematically studied. Apparently, the first stage of such a multi-disciplinary investigation is to seasonally map the air concentrations of anthropogenic pollutants over open sea areas. Consequently, the main aim of the present study is to perform contemporary open sea and coastal aerosol monitoring and evaluation with the assistance of a set of complementary experimental and model methods. By this approach, it is expected to get a more accurate insight into the seasonal chemical inventory of ship emission released aerosols on the southern North Sea.

2. Experimental

2.1. Sampling areas, campaigns and meteorological data collection

Six sampling campaigns, each being ten-day-long, have been carried out onboard the research vessel R/V Belgica during different seasons in 2010 (May 3–12, September 6–16, October 4–15) and in 2011 (January 31–February 11, March 14–25, May 16–27), excluding the weekends. The sampled marine areas covered the main ship routes of the southern

North Sea (Fig. 1), e.g., main international, west-east route to Zeebrugge and the Scheldt estuary, or out of the ship lanes to collect background (BG) pollution samples/data. The geo-coordinates of the examined marine areas and the meteorological parameters on routes of the R/V Belgica along with the ground speed of the ship, the relative/real wind speed, and the ship-heading have been recorded by the On-board Data Acquisition System (ODAS) and presented in detail in the corresponding cruise reports (MUMM, 2020). Accordingly, air temperature, air pressure, relative humidity (RH), wind speed (WS), wind direction, precipitation, solar radiation and sea water temperature were recorded. In this study, the term “open sea” is used in a broader context, corresponding to marine areas off the coastal waters, e.g., farther than 1 km of the Belgian coastline of the North Sea.

In addition to marine sampling campaigns, concurrent samplings were conducted at a coastal BG site in De Haan, Belgium, located at geo-coordinates of 51.28688° N and 3.06098° E, which is a small research station of the Flanders Marine Institute (Vlaams Instituut voor de Zee – VLIZ). The site is located around 500 m from the coastline among the sand-dunes, which form a characteristic pattern for the coast of the southern North Sea. Similarly as for onboard samplings, the meteorological parameters were registered concurrently at the coastal research station. For this purpose, a small weather unit, which logged the data with a second frequency, was installed by VLIZ. As an alternative, the weather data were obtained from the extensive database of the Monitoring Network of the Flemish Banks (MVB, 2020). The meteorological conditions were evaluated for the sampled open sea and coastal environment for the seasons and the sampling campaigns/cycles to get an insight on the representativeness of the weather parameters observed for an individual campaign and the corresponding season.

2.2. Sampling and monitoring methods

Gaseous nitric acid, nitrous acid and ammonia were sampled actively from the ambient air with an URG-2000-01K annular denuder at 10 dm³/min during each sampling campaign. The denuder tubes were coated with a 1:1 diluted methanolic solution of 1% (m/v) sodium carbonate plus 1% (v/v) glycerol and 1% (m/v) citric acid plus 1% (v/v) glycerol in methanol for the collection of acidic and alkaline gases, respectively.

Particulate matter (PM) in the size-ranges of PM₁, PM_{2.5} and PM₁₀ was simultaneously collected with the use of three pairs of Harvard-impactors and vibrating diaphragm pumps (MS&T™ Air Diagnostics and Engineering Inc., Harrison, ME, USA). As collecting substrates for PM, Pallflex type TK15-G3M membrane filters (Pall Life Sciences, Ann Arbor, MI, USA) with 37 mm diameter and 0.3 μm pore size were applied on each impactor plate. The impactor units were attached through plastic tubing to the pumps, which maintained constant air-flow rates (PM₁: 23 dm³/min, PM_{2.5} and PM₁₀: 10 dm³/min). The sampled air volume was registered with Gallus-2000 gas meters, while a calibrated rotameter was applied regularly to check the air flows of the pumps before and after each sampling cycle.

Each membrane filter was weighed on a Sartorius Model M5P-000V001 microbalance (Göttingen, Germany) before and after sampling, according to the EN12341 protocol in a thermostated room with a temperate air of 20 °C and at RH of 50%. The mass concentrations for PM_{10-2.5} and PM_{2.5-1} fractions, further on referred to as coarse aerosol and medium-sized aerosol, respectively, were calculated from the difference in masses between the three sampled aerosol fractions. Thereafter, the aerosol-loaded and field blank filters were subjected to energy-dispersive X-ray fluorescence (EDXRF) and ion chromatography (IC) analysis, as described in detail elsewhere (Van Meel et al., 2010; Bencs et al., 2017).

Equivalent black carbon (BC) content of atmospheric air was monitored at 1 min frequency with a portable Model AE-42 Aethalometer (Magee Scientific, Berkeley, CA, USA). The air-flow rate was set at 3.9 dm³/min. This instrument facilitates the combination of optical

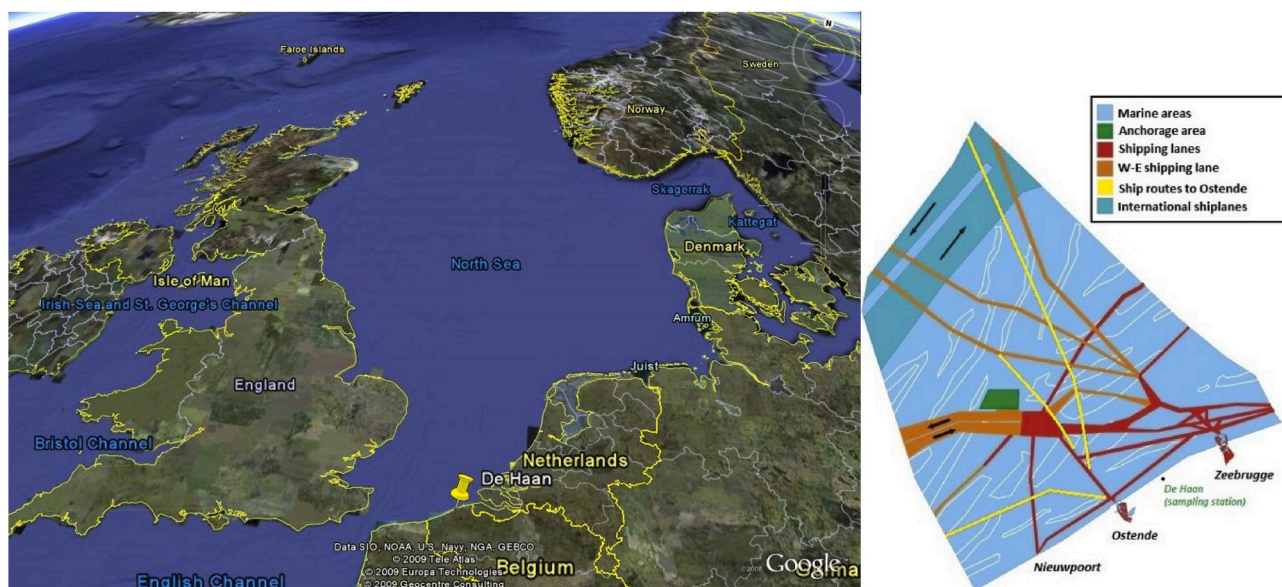


Fig. 1. Map of the North Sea (main graph) and the enlarged schematic of the Belgian Continental Shelf (auxiliary graph) with the main national and international shipping lanes, the major Belgian harbors, the sand reefs (Flemish Banks) and the coastal background station (De Haan).

absorption measurements at wavelengths of 880 nm for BC aerosol and at 370 nm designated as UVP. The latter is interpreted as an indicator of UV-absorbing organic particulates, for instance, aromatic organic compounds (e.g., PAHs) and recorded also as “equivalent BC” concentration. The seasonal and site-specific averages of the BC concentrations were calculated for PM_{10} and taken into account in the mass closure evaluations.

The sampling equipment, used onboard R/V *Belgica*, were deployed on the foredeck, in front of the bridge. The inlet of the sampling tube for the BC monitor was fixed at the monkey-bridge, whereas the instrument itself was placed and fixed inside the bridge. The sampling equipment was switched off for short periods of time, when the ships’ own plumes were expected to affect the sampling, e.g., during turning maneuvers when the front and stern of the ship crossed the direction of the wind.

2.3. Sample preparation

For IC analysis, the membrane filters were exposed to ultrasonic aided leaching in 5 ml ultrapure (Milli-Q) water and the leachate solutions were analyzed for their cationic and anionic content by means of IC. For the analysis of gaseous hydrochloric acid, sulfur dioxide, nitric acid, nitrous acid and ammonia, the absorber-tubes of the denuders were eluted with 10 ml Milli-Q water and the leachate solutions were subsequently analyzed with IC for their Cl^- , SO_4^{2-} , NO_2^- , NO_3^- and NH_4^+ content. The air concentration of the corresponding pollutant was calculated by taking into account the sampled air volume.

2.4. Mass closure calculation and statistical methods

The water-soluble (ionic) compositions of aerosols were evaluated on the basis of the method of chemical boundary conditions (CBC), which utilizes a couple of fundamental (e.g., acidic-basic) chemical reactions occurring in the troposphere (Anaf et al., 2012, 2013). The water content of the ionic aerosol components was assessed by applying the single-parameter estimation method of Kreidenweis et al. (2008). In part of these calculations, the aerosol density data reported by Zelenyuk et al. (2005) were utilized. The mineral content of aerosols was evaluated from the concentrations of individual soil components (e.g., Al, Si, Ca, Fe, Ti) determined in PM, as described elsewhere (IMPROVE, 2020). The data for each quantitated aerosol component (ionic constituents, BC, elemental and mineral content) was clustered according to the season

and subsequently applied in the chemical mass closure calculations.

3. Results and discussion

3.1. Summary of meteorological conditions

The weather parameters evaluated for various periods of the marine and coastal sampling campaigns in 2010 and 2011 are depicted in Fig. S1. The coastal and the open sea campaigns experienced similar weather conditions, apart from the wind speed, which is certainly higher on the open sea. The weather data for the campaigns showed very similar absolute values and periodicity to those observed on a yearly basis, monitored at an official weather station at the coast of Zeebrugge, located about 12 km NNE of De Haan (Fig. S3). These data and their fluctuations are in accordance with the Köppen-classification of oceanic climate (“Cfb”) for the study region. Specifically, solar radiation, air temperature and sea water temperature were peaking in the warm season and reaching their minimum in the cold season. On the other hand, the RH peaked in winter and showed the minimum in summer, in the range of 75–90% with fairly high (10–15%) fluctuations in each season. In the current sampling campaigns, the prevalence of marine (oceanic or North Sea) winds was experienced at the coastal research station (Fig. S2). Certainly, the wind speed logged at the coast was lower by 20–30% than those observed during the open sea campaigns, mostly due to the shielding effects of the sand dunes for the coastal station. On the basis of these observations, the general tendency of the marine air pollutants released by ocean-going ships is to proceed towards the shores of the southern North Sea, where they mix with pollutants from local, anthropogenic sources and apparently increase the extent of coastal air pollution.

3.2. Variation of aerosol mass concentration and size-distribution

The mass concentration of coarse aerosol ($PM_{10-2.5}$) suspended in marine air (Fig. 2) is higher or of similar level (range: 7.4–18 $\mu g/m^3$; average: 12.3 $\mu g/m^3$; median: 12.0 $\mu g/m^3$), compared to that sampled at the coastal station (range: 6.9–15.2 $\mu g/m^3$; average: 10.2 $\mu g/m^3$; median: 9.2 $\mu g/m^3$). From May 2010, an increase is seen in the mass concentration of coarse PM, although it shows rather fluctuating values during the subsequent winter. On the other hand, the PM_{10} concentration was gradually increasing from late spring (May 2010) till end of the

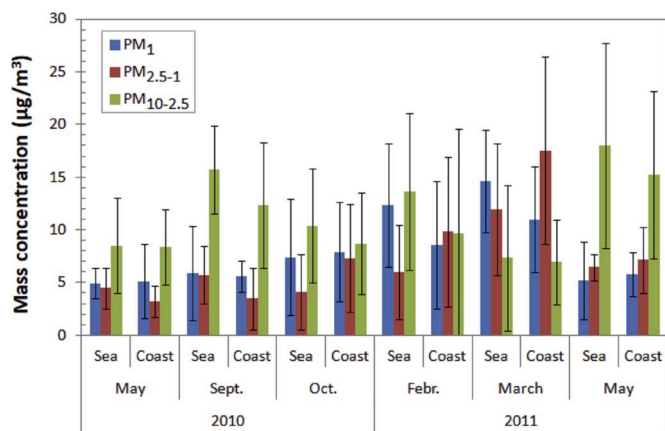


Fig. 2. Seasonal variation of the average mass concentrations of PM fractions over the southern North Sea and at the coastal background site (De Haan, Belgium) in sampling campaigns of 2010 and 2011; error bars denote the ranges for within season fluctuations.

winter (March 2011), i.e., from 18 to 35 µg/m³.

Interestingly, the mass concentration of the medium aerosol fraction (PM_{2.5-1}) on the open sea showed a gradual increase during the cold season (i.e., from October 2010 till March 2011), ranging from 4.1 to 12 µg/m³, which is a similar trend to that observed for PM₁₀. A similar pattern, but with slightly higher values could be seen for coastal aerosol (range: 7.3–17.5 µg/m³) during the same season. Whilst again, in May 2011, the mass concentration of medium aerosol fraction fell to the level observed in the same season (spring-summer) of the previous year, 2010. The average marine PM₁ mass (range: 4.9–14.6 µg/m³; average: 8.4 µg/m³; median: 6.7 µg/m³) has been found to follow a similar seasonal trend as the medium-sized aerosol fraction. Fine aerosol (PM₁)

sampled at the coastal site has shown similar seasonal trends, but with slightly lower values (range: 5.1–11 µg/m³; average: 7.3 µg/m³; median: 6.9 µg/m³).

It is also apparent that the coarse mass fraction dominates over the medium and the fine fractions during the spring and early autumn (May–September campaigns), whereas the fine and medium fractions are generally represented by higher aerosol masses during winter/early spring (February/March 2011). Exception is the March 2011 campaign, when the medium-size and fine aerosol fraction dominated in the coastal and marine sites, respectively.

It is important to emphasize that the mass concentrations of the coarse (PM_{10-2.5}) and fine (PM₁) marine aerosols are higher than those sampled at the coastal site, while for the medium-size fraction (PM_{2.5-1}) the trend is usually opposite. For open sea aerosols, the increased mass concentration in the fine fraction unambiguously points towards its source from ship-exhaust emissions, while the increased mass in the coarse and the decreased mass in the medium-size fractions show faster coagulation of medium-sized aerosols (compared to those of fine particulates), which is likely due to the higher humidity condition that exists in general over marine areas. Unexpectedly, seasonal differences can be noticed when comparing the spring and autumn campaigns in 2010. Namely, increased aerosol masses at each size fraction could be seen for the autumn samples.

3.3. Elemental content and seasonality of size-segregated aerosols

The concentrations of minor elements are rather fluctuating over various campaigns/seasons (Fig. 3). Here, the “Trace” content refers to the summed concentrations of the detected trace elements, whose average concentration does not reach 100 ng/m³ in either size fraction. The highest levels are experienced for aerosol Cl mostly in the coarse fractions of marine samples (range: 0.76–3.2 µg/m³; average: 1.97 ±

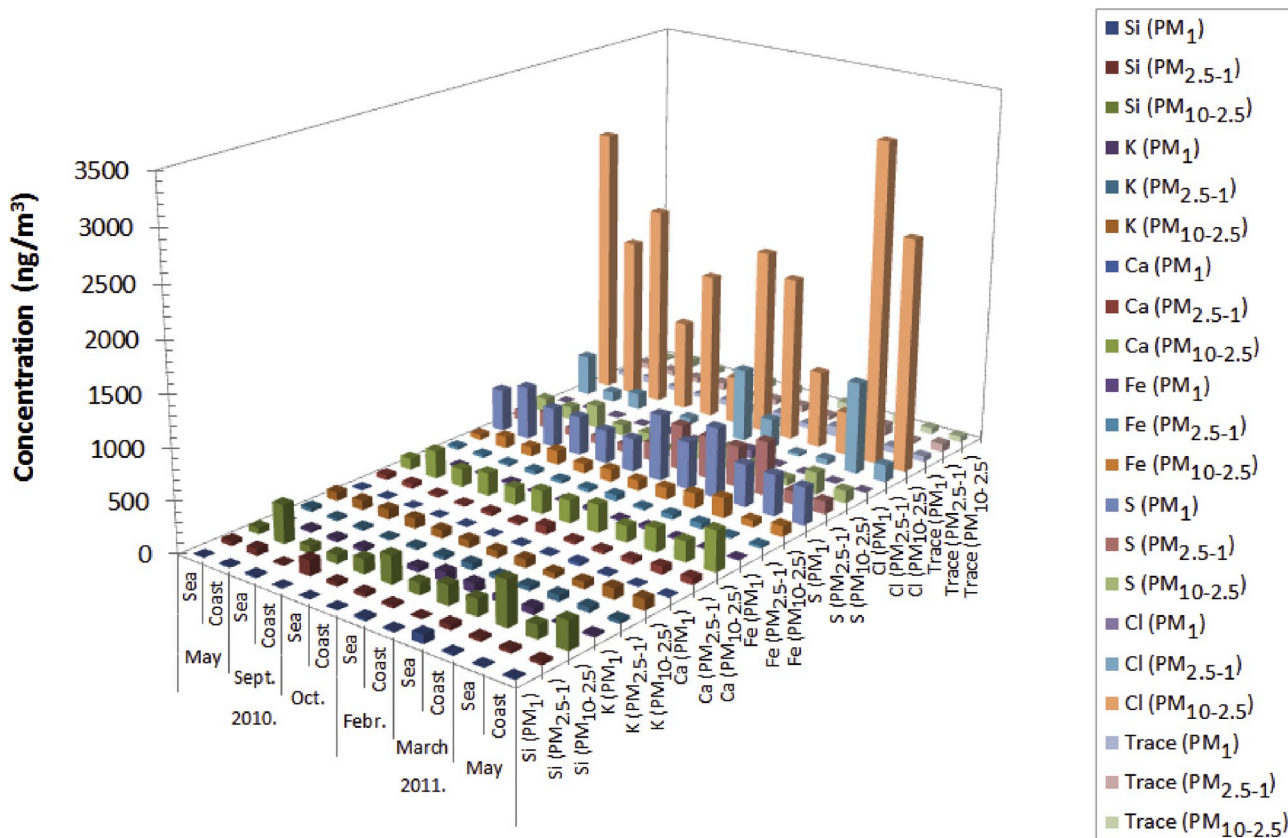


Fig. 3. Concentrations of minor and trace elements in various fractions of marine aerosols (“Trace” denotes the trace element content – detailed in Fig. 4).

0.86 $\mu\text{g}/\text{m}^3$; median: 1.9 $\mu\text{g}/\text{m}^3$), while its decreasing contribution has been found in medium-sized aerosols (range: 0.29–0.9 $\mu\text{g}/\text{m}^3$; average: $0.38 \pm 0.36 \mu\text{g}/\text{m}^3$; median: 0.28 $\mu\text{g}/\text{m}^3$), as well as in fine PM (range: 0.003–0.015 $\mu\text{g}/\text{m}^3$; average: $0.009 \pm 0.004 \mu\text{g}/\text{m}^3$; median: 0.009 $\mu\text{g}/\text{m}^3$). The aerosol Cl was always higher in coarse and medium-sized marine aerosols, while interestingly, higher Cl levels were experienced in fine fraction of coastal PM. For aerosol S, the trend is rather the opposite than that observed for Cl. The concentration of S peaked in fine PM, in marine aerosols it covered the range of 0.33–0.69 $\mu\text{g}/\text{m}^3$ (average: $0.48 \pm 0.15 \mu\text{g}/\text{m}^3$; median: 0.41 $\mu\text{g}/\text{m}^3$), while for coastal samples, its level was just slightly lower (range: 0.33–0.52 $\mu\text{g}/\text{m}^3$; average: $0.41 \pm 0.07 \mu\text{g}/\text{m}^3$; median: 0.40 $\mu\text{g}/\text{m}^3$). Medium-sized PM showed a lower S content than fine PM, but considerably higher fluctuations. For instance, for marine aerosols, it ranged between 0.075–0.45 $\mu\text{g}/\text{m}^3$ (average: $0.21 \pm 0.17 \mu\text{g}/\text{m}^3$; median: 0.11 $\mu\text{g}/\text{m}^3$), while for coastal samples, it was a bit higher, ranging between 0.077–0.54 $\mu\text{g}/\text{m}^3$ (average: $0.25 \pm 0.18 \mu\text{g}/\text{m}^3$; median: 0.17 $\mu\text{g}/\text{m}^3$). It could be seen that the aerosol S level rather increased during the cold season (February/March campaigns) in both the fine and the medium-size PM fractions. In general, significantly lower S content was experienced in coarse marine aerosols (range: 0.1–0.22 $\mu\text{g}/\text{m}^3$; average: $0.16 \pm 0.05 \mu\text{g}/\text{m}^3$; median: 0.15 $\mu\text{g}/\text{m}^3$), while only a slightly lower S level

was obtained at the coastal site (range: 0.02–0.2 $\mu\text{g}/\text{m}^3$; average: $0.11 \pm 0.06 \mu\text{g}/\text{m}^3$; median: 0.11 $\mu\text{g}/\text{m}^3$). For coarse S, the seasonal change is not so obvious. In coarse marine aerosols, peaks of S-content have been observed in the September 2010 and May 2011 campaigns, while for coastal aerosols in February, each around 0.2 $\mu\text{g}/\text{m}^3$.

Crustal (mineral) elements, such as Al, Ca, Fe, Si and Ti, were more apparently dominating in coarse aerosols (Figs. 3 and 4), covering the concentration range of 16–42 ng/m^3 (average: $25 \pm 11 \text{ng}/\text{m}^3$; median: 24 ng/m^3), 109–223 ng/m^3 (average: $172 \pm 39 \text{ng}/\text{m}^3$; median: 171 ng/m^3), 53–149 ng/m^3 (average: $93 \pm 33 \text{ng}/\text{m}^3$; median: 94 ng/m^3), 62–166 ng/m^3 (average: $115 \pm 40 \text{ng}/\text{m}^3$; median: 123 ng/m^3) and 2.3–8.8 ng/m^3 (average: $5.2 \pm 2.4 \text{ng}/\text{m}^3$; median: 5.1 ng/m^3), respectively, over marine areas. At the coastal site, significantly higher air levels of these elements were usually observed as compared to concentrations obtained over marine areas, indicating the terrestrial, upper soil/dust origin. However, for the medium-sized fraction, the concentration trend is less obvious. For Si, generally lower, or similar levels in marine and coastal $\text{PM}_{2.5-1}$ could be observed, except for the winter, when a three times higher Si content was found over marine areas. For Ca, Fe and Ti, higher levels were observed in winter, while lower values were recorded for Al in the same season. For fine PM, Al, Ca, Fe, Si and Ti were present at enhanced levels in the cold season (February and

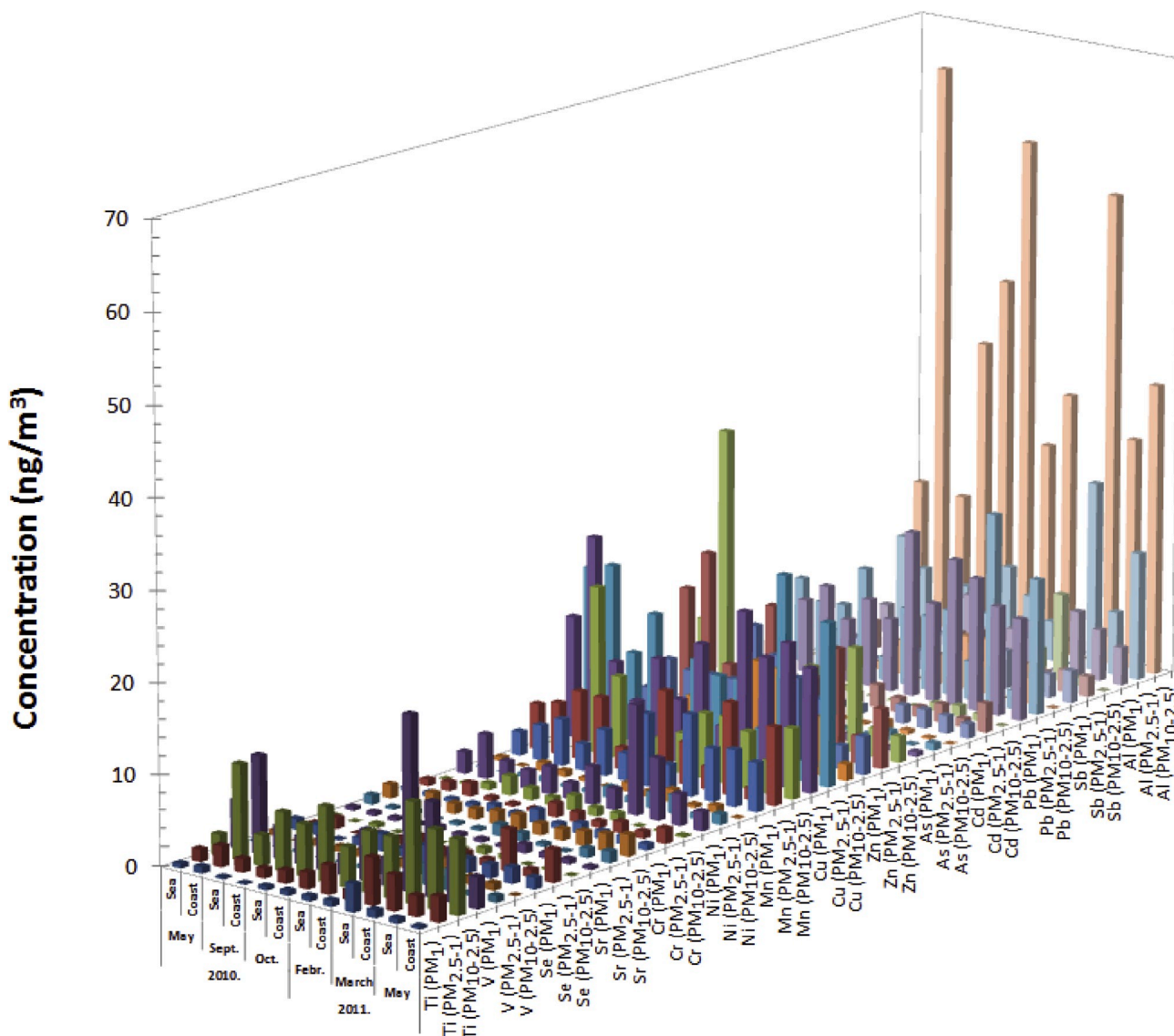


Fig. 4. Concentration distribution of trace elements in marine and coastal aerosols over various campaigns/seasons.

March), whereas, their distribution did not show any visible trend over the studied marine areas, nor the coastal sampling station.

Potassium was present at increased amounts in coarse marine aerosols (range: 53–107 ng/m³, average: 82 ± 19 ng/m³, median: 82 ng/m³), but its concentration did not show significant deviation from the coastal data, nor much seasonality (Fig. 3). About half of the aerosol K was found in the medium-size fraction (range: 21–60 ng/m³ average: 39 ± 14 ng/m³, median: 39 ng/m³), as well as in fine PM (range: 13–97 ng/m³ average: 44 ± 31 ng/m³, median: 38 ng/m³). It can be seen that this element rather occurs at enhanced levels during winter at the coastal station too. This could be due to biomass burning and/or wood heating activities at nearby settlements.

Fine aerosol related V and Ni are excellent indicators of residual (diesel) oil burning (Maenhaut et al., 2002), as well as ship emissions (Viana et al., 2009). In this study, these elements were more concentrated in the cold season and in fine PM. Over marine areas, the V and Ni content of PM₁ fluctuated in ranges of 3.7–19.3 ng/m³ (average: 7.3 ng/m³, median: 5.5 ng/m³) and 2.4–12.2 ng/m³ (average: 4.6 ng/m³, median: 3.3 ng/m³), respectively (Fig. 4). The V and Ni levels in coastal fine aerosols ranged at 2.3–10.8 ng/m³ (average: 5.5 ng/m³, median: 3.3 ng/m³) and 1.8–6.9 ng/m³ (average: 3.4 ng/m³, median: 2.2 ng/m³), respectively. Both elements contributed rather equally low to medium-sized and coarse PM, ranging between 0.2–2.4 and 0.3–2.1 ng/m³, respectively, over the sampling sites and seasons. These findings point towards their origin from ship emissions. Pb has shown a similar seasonal pattern in fine PM, ranging from 5.1 to 18.7 ng/m³ (average: 12.2 ng/m³) and 7–15 ng/m³ (average: 10.2 ng/m³), over marine sites and the coastal station, respectively. For marine aerosols, the Pb level showed a gradually decreasing trend towards the coarser PM fractions, e.g., with averages of 5.8 and 3.6 ng/m³, in PM_{2.5-1} and PM_{10-2.5}, respectively. Whereas, at the coastal station, its level in medium-sized PM was similar or slightly higher than that observed in the fine fraction, ranging from 7.4 to 21 ng/m³ (average: 12.5 ng/m³).

Elements like Cu, Mn and Zn in marine aerosols were found to be at similarly low concentrations in the studied PM fractions (Fig. 4). Evidently, their levels in fine PM ranged from 2.6 to 9.1 ng/m³ (average: 6.1 ng/m³), 9.6–18.5 ng/m³ (average: 13.8 ng/m³), and 2.7–13.9 ng/m³ (average: 7.4 ng/m³), respectively. On average, about 20–30% lower levels were found in coastal fine PM. In the medium fractions of marine aerosols, the levels of Cu and Mn were observed to be similar to those found for each in fine PM, ranging from 1.4 to 9.9 ng/m³ (average: 4.8 ng/m³) and 2.3–18.5 ng/m³ (average: 7.9 ng/m³), respectively. In coarse marine aerosol, generally, lower Cu and Zn content was obtained, fluctuating between 1.8 and 10.8 ng/m³ (average: 6.2 ng/m³) and 2.2 and 11.2 ng/m³ (average: 5.6 ng/m³), whereas higher Mn levels were attained, ranging from 3.7 to 18.7 ng/m³ (average: 7.9 ng/m³). In coastal PM, usually, higher Mn and Zn levels were obtained in the coarse fractions, whereas the Cu content decreased in coarse aerosol (range: 0.5–11.2 ng/m³, average: 4.0 ng/m³).

Chromium in marine fine PM followed a similar seasonal pattern to Pb. Namely, its level increased by 2–3 fold in the cold season, when fluctuating between 0.4 and 1.5 ng/m³ (average: 0.9 ng/m³), whereas slightly lower Cr levels were detected at the coastal station (range: 0.4–0.9 ng/m³, average: 0.6 ng/m³). Interestingly, this element was rather homogeneously distributed between the three particulate fractions in marine samples, while in coastal samples, the medium and coarse fractions showed twice higher levels than that present in fine PM. Other trace elements, like As, Cd, Sb and Se showed similarly low (a few ng/m³) levels on average, in each PM fraction, as compared with that of Cr, as well as similar seasonality in terms of enhanced concentrations during the cold season (Fig. 4). Each element followed a decreasing concentration trend from fine to coarser PM fractions in marine aerosol, whereas the trend was not so discernible for coastal samples, which were usually characterized with higher levels of these elements in the coarser fractions. The average As, Cd, Sb and Se content in fine PM ranged in 0.2–0.9 ng/m³ (over seasons average: 0.5 ng/m³), 0.1–2.1 ng/m³

(average: 1.3 ng/m³), not detectable (n.d.) - 4.3 ng/m³ (average: 0.5 ng/m³), and 0.1–1.9 ng/m³ (average: 1.4 ng/m³), respectively. Although similarly low levels to these were observed for Sr, its distribution over the three aerosol fractions was reverse compared to the above mentioned elements, in terms of its gradually growing concentration from the fine to the coarse fraction. Sr is likely of marine spray or terrestrial (crustal) origin, thus its higher abundance in the coarser aerosol fractions is more evident.

3.4. Seasonal changes in air levels of ammonia and acidic gases

The total (summed, daily) concentration of the monitored gaseous species (HNO₂, HNO₃, HCl, SO₂, NH₃) fluctuated between 0.6 and 15 µg/m³ over the marine sampling campaigns/seasons (Fig. 5). The air level of NH₃ was the highest among these gases, ranging between 0.4 and 9.5 µg/m³, followed by gradually lower air levels of HNO₂, HCl, HNO₃ and SO₂. High concentrations of NH₃ were observed in the spring season in May, both in 2010 and 2011, but also in March 2011, reaching about 3 µg/m³. The air level of HNO₂ was found to be rather high in the autumn/winter periods, e.g., in September 2010, February–March 2011 campaigns, peaking at about 0.9 µg/m³. Interestingly, in March 2011, rather high NH₃ and HNO₂ levels were seen. During this campaign, the weather was characterized by fairly wind-calm conditions, as well as frequent and dense fog events with highly limited sunny hours (Fig. S1), which could have contributed to the accumulation of the reduced forms of N-species in the North Sea air. On the other hand, HNO₃ and HCl peaked at 0.8 and 1.3 µg/m³ during the May and October campaigns in 2010, respectively. Gaseous HCl is most likely formed during conversion of sea spray, which loses chloride in reaction with acidic gases soon after formation on the open sea, hence, partly converted sea salt aerosols are expected in the coastal air. Similar observations were made earlier for the coastal North Sea (Horemans et al., 2009).

The maxima of the total gaseous pollutant concentrations were observed during the cold season between October 2010 and March 2011 (Fig. 5). In winter, more diesel fuel is consumed by ocean-going vessels than during summer, due to the cold start of the ships' primary engines at harbors and mooring areas, and likely the need of more power for ship safety/navigation systems and heating. It is also likely that the catalytic

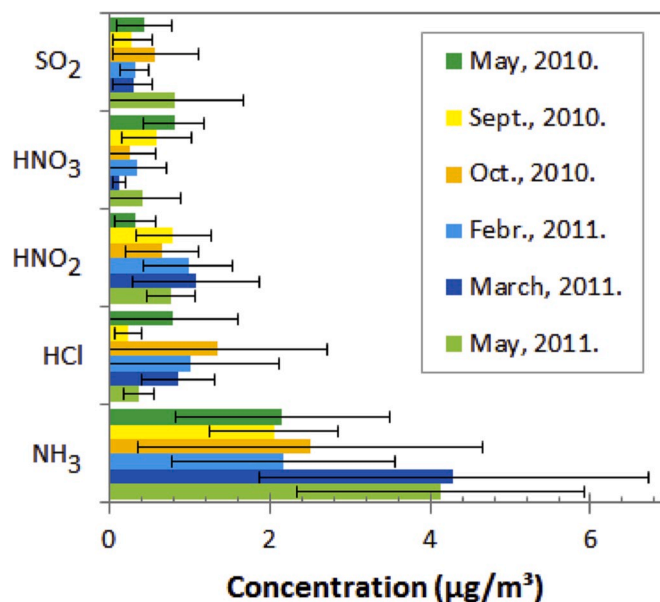


Fig. 5. Seasonal variation in the average concentrations of gaseous air-pollutants over open sea areas and the corresponding within campaign fluctuations expressed as error bars (similar seasons are indicated with similar colours). (For interpretation of the references to colour in this figure legend, the reader is referred to the Web version of this article.)

converters of the ship's engines reach the maximum conversion efficiency more slowly in winter than during the warm season. These conditions result in higher gaseous pollutant emissions into the North Sea air in winter, and apparently more intense formation of secondary aerosol, thus higher contribution of anthropogenic particulate to the total aerosol mass. Moreover, the weather conditions can also contrast the seasonal differences in air pollution levels, due to less wind and calm seas during the winter period, which can promote accumulation of these species in the ambient air.

3.5. Seasonal changes in water-soluble components of size-segregated aerosols

Interestingly, the total (sum) of ionic species is generally higher for samples collected on the open sea than those at the coastal monitoring station (Fig. 6). The temporal trends of total ionic concentrations

sampled on the sea and at the coastal station were found to be very similar to the pattern of the PM mass concentration, i.e., increasing levels from late spring towards the cold season, and reaching peak values in February/March 2011.

From the results, it is apparent that genuine sea salt is more abundant in the coarse particulate fraction ($PM_{10-2.5}$), showing concentrations from 1.9 to 7.0 $\mu\text{g}/\text{m}^3$ (average: 4.3 $\mu\text{g}/\text{m}^3$) and 1.1–5.1 $\mu\text{g}/\text{m}^3$ (average: 2.7 $\mu\text{g}/\text{m}^3$), respectively, for marine and coastal BG samples. In general, much lower levels have been observed in medium size-ranged aerosols, in concentrations from 0.35 to 1.5 $\mu\text{g}/\text{m}^3$ (average: 0.75 $\mu\text{g}/\text{m}^3$) and 0.18–1.05 $\mu\text{g}/\text{m}^3$ (average: 0.53 $\mu\text{g}/\text{m}^3$), respectively, for marine and coastal aerosols, whereas in PM_1 fraction, the sea salt concentration was negligibly low for both the sea areas and the coastal sites, ranging from 0.11 to 0.67 $\mu\text{g}/\text{m}^3$ (average: 0.3 $\mu\text{g}/\text{m}^3$) and from 0.04 to 0.11 $\mu\text{g}/\text{m}^3$ (average: 0.08 $\mu\text{g}/\text{m}^3$), respectively (Fig. 6). Genuine sea salt peaked rather in the spring or early autumn, in fine, medium and coarse

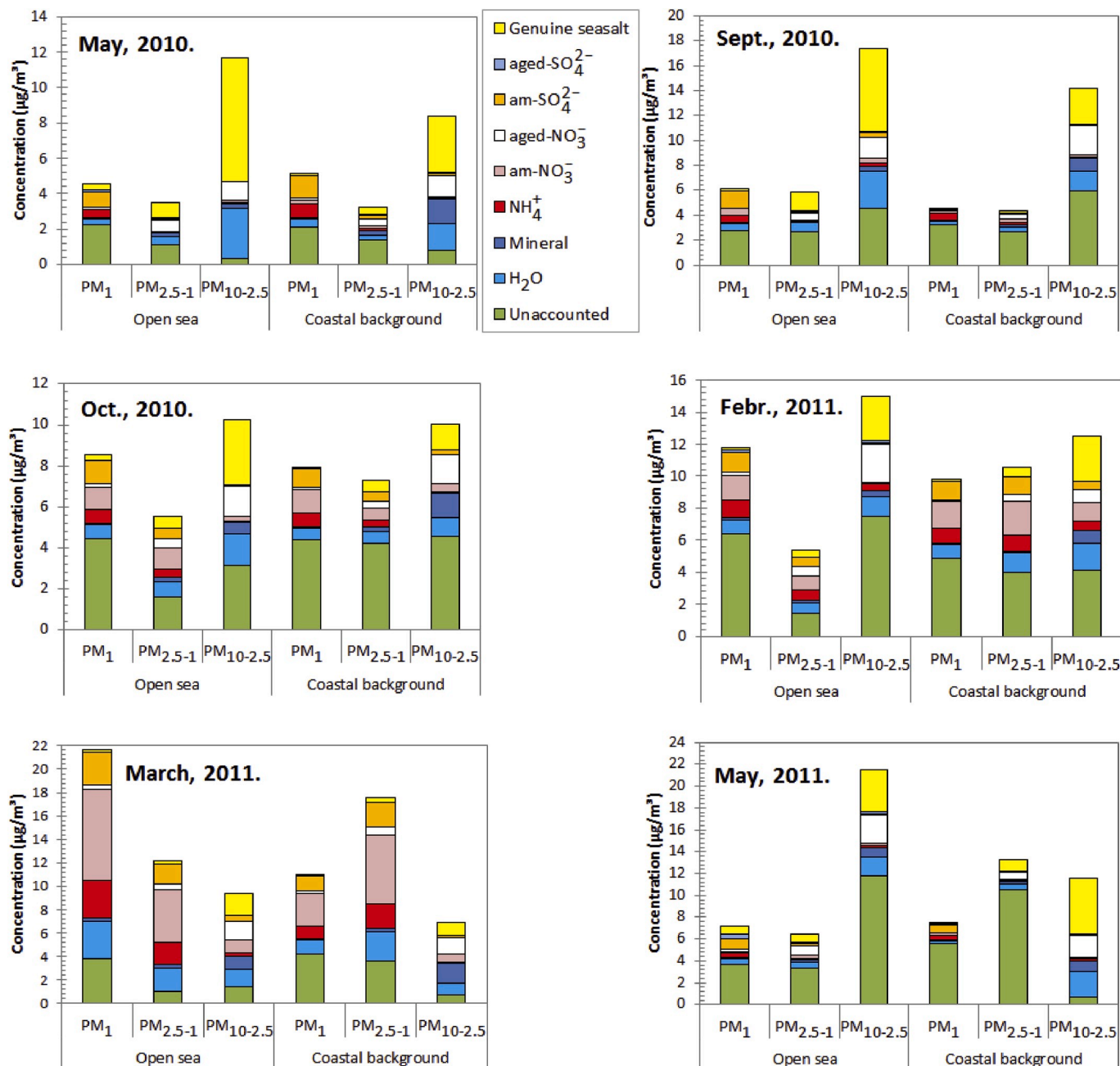


Fig. 6. Concentration variation of ionic species, mineral and water content from open sea and coastal background aerosols in various campaigns/seasons.

fractions of the marine aerosols. However, for coastal fine and medium-sized aerosols, it was rather high in winter, whereas its maximum in coarse aerosols was found in the warmer, late spring season (e.g., May 2011).

Aged sea salt bound SO_4^{2-} content in marine fine aerosols ranged widely, from n.d. to $0.49 \mu\text{g}/\text{m}^3$ (average: $0.3 \mu\text{g}/\text{m}^3$), whereas in coastal fine PM, it was much lower, ranging from 0.001 to $0.07 \mu\text{g}/\text{m}^3$ (average: $0.02 \mu\text{g}/\text{m}^3$). In medium-sized marine aerosols, its concentration was slightly higher, ranging from 0.01 to $0.12 \mu\text{g}/\text{m}^3$ (average: $0.05 \mu\text{g}/\text{m}^3$), while in the corresponding coastal samples it was slightly lower, i.e., ranged from 0.002 to $0.09 \mu\text{g}/\text{m}^3$ (average: $0.03 \mu\text{g}/\text{m}^3$). In coarse PM, aged SO_4^{2-} was lying in the range of n.d.- $0.21 \mu\text{g}/\text{m}^3$ (average: $0.08 \mu\text{g}/\text{m}^3$), while in coastal PM, it was lower than the marine values, ranging from 0.01 to $0.07 \mu\text{g}/\text{m}^3$ (average: $0.05 \mu\text{g}/\text{m}^3$). As for seasonal differences, the increase for sea salt bound fine SO_4^{2-} is towards the spring (May 2010 and 2011) in both the marine and the coastal samples. This observation is partly true for medium-sized and coarse aerosols; they also mostly peak in the spring, as well as in the late winter (February 2011).

The concentration of sea salt bound NO_3^- (aged sea salt) in fine aerosols was lying generally in a similar range than that of the former species, i.e., for marine aerosols, between 0.08 and $0.42 \mu\text{g}/\text{m}^3$ (average: $0.21 \mu\text{g}/\text{m}^3$), while in coastal aerosols between 0.08 and $0.74 \mu\text{g}/\text{m}^3$ (average: $0.22 \mu\text{g}/\text{m}^3$). In medium-size marine aerosols, it showed a considerable increase, compared to fine PM, ranging between 0.47 and $0.82 \mu\text{g}/\text{m}^3$ (average: $0.59 \mu\text{g}/\text{m}^3$), while it was slightly lower in coastal samples, covering the range between 0.08 and $0.66 \mu\text{g}/\text{m}^3$ (average: $0.37 \mu\text{g}/\text{m}^3$). As expected, the main mass of sea salt bound NO_3^- was observed in coarse aerosols, for both marine and coastal samples, ranging between 1.0 and $2.5 \mu\text{g}/\text{m}^3$ (average: $1.8 \mu\text{g}/\text{m}^3$), and between 0.03 and $2.3 \mu\text{g}/\text{m}^3$ (average: $1.2 \mu\text{g}/\text{m}^3$), respectively. Seasonally, the sea salt bound fine NO_3^- (aged sea salt) peaked in the cold season (February 2011) for marine areas, whereas interestingly, it was peaking in spring (May 2011) at the coastal station. A similar trend was observed for sea salt bound medium-size NO_3^- found in marine samples, which peaked in spring (May 2010) and winter (February 2011), while for the coastal site, its maximum was observed clearly in the cold season. Similarly, the sea salt bound coarse NO_3^- peaked in spring for marine areas (May 2010 and 2011), whereas, interestingly, it peaked in autumn (September 2011) in coastal samples.

Ammonium-bound SO_4^{2-} levels in marine fine aerosols generally ranged from 0.89 to $2.7 \mu\text{g}/\text{m}^3$ (average: $1.4 \mu\text{g}/\text{m}^3$), while in fine coastal aerosols, it reached significantly lower values, ranging from 0.20 to $1.3 \mu\text{g}/\text{m}^3$ (average: $0.99 \mu\text{g}/\text{m}^3$). In medium-sized marine aerosols, the concentration of ammonium-bound SO_4^{2-} was about 2-3-times lower than in fine PM, i.e., ranging from 0.09 to $1.64 \mu\text{g}/\text{m}^3$ (average: $0.51 \mu\text{g}/\text{m}^3$), whereas in coastal samples it reached slightly higher values, i.e., between 0.08 and $2.14 \mu\text{g}/\text{m}^3$ (average: $0.75 \mu\text{g}/\text{m}^3$). In coarse marine PM, aged SO_4^{2-} was found to be at very low levels, e.g., from n.d. to $0.43 \mu\text{g}/\text{m}^3$ (average: $0.16 \mu\text{g}/\text{m}^3$), while in coastal PM, it was slightly higher, ranging from 0.11 to $0.51 \mu\text{g}/\text{m}^3$ (average: $0.22 \mu\text{g}/\text{m}^3$). Seasonally, ammonium-bound SO_4^{2-} peaked in the cold season (March 2011) for all the three studied aerosol fractions over marine sites, as well as similar seasonal trends could be observed for the coastal aerosols.

The ammonium-bound NO_3^- content in marine fine aerosols ranged widely, i.e., from 0.04 to $7.8 \mu\text{g}/\text{m}^3$ (average: $1.8 \mu\text{g}/\text{m}^3$), whereas in fine coastal aerosols it reached significantly lower values, ranging from 0.22 to $2.8 \mu\text{g}/\text{m}^3$ (average: $1.1 \mu\text{g}/\text{m}^3$). In medium-sized marine aerosols, the ammonium-bound NO_3^- content was about half lower than in marine fine PM, i.e., ranging from 0.003 to $4.4 \mu\text{g}/\text{m}^3$ (average: $1.1 \mu\text{g}/\text{m}^3$), whereas in coastal samples it reached slightly higher values, i.e., 0.07– $5.9 \mu\text{g}/\text{m}^3$ (average: $1.5 \mu\text{g}/\text{m}^3$). In coarse marine PM, the ammonium-bound NO_3^- was found to be at relatively lower levels, as compared to the fine and medium-sized fractions, fluctuating from 0.02 to $1.1 \mu\text{g}/\text{m}^3$ (average: $0.36 \mu\text{g}/\text{m}^3$), while in coastal PM, it was present at slightly higher levels, between 0.05 and $1.14 \mu\text{g}/\text{m}^3$ (average: 0.44

$\mu\text{g}/\text{m}^3$). As for seasonal differences, similarly to the ammonium-bound SO_4^{2-} , the ammonium-bound NO_3^- reached the maximum levels in the cold season (March 2011) for the three studied aerosol fractions over marine sites, while a similar seasonal trend was observed for the coastal samples.

The NH_4^+ content in marine fine aerosols fluctuated widely, i.e., from 0.4 to $3.2 \mu\text{g}/\text{m}^3$ (average: $1.1 \mu\text{g}/\text{m}^3$), whereas in coastal fine aerosols it was represented with significantly lower values, ranging from 0.08 to $1.2 \mu\text{g}/\text{m}^3$ (average: $0.69 \mu\text{g}/\text{m}^3$). The NH_4^+ content in medium-sized marine aerosols was around twice lower than in the marine fine particulate, ranging between 0.04 and $1.9 \mu\text{g}/\text{m}^3$ (average: $0.5 \mu\text{g}/\text{m}^3$), whereas in coastal samples it reached slightly higher values, e.g., 0.16– $2.0 \mu\text{g}/\text{m}^3$ (average: $0.74 \mu\text{g}/\text{m}^3$). In coarse marine aerosols, the NH_4^+ content was found to be at quite lower levels, as compared to the fine and medium-sized fractions, i.e., ranging from 0.03 to $0.45 \mu\text{g}/\text{m}^3$ (average: $0.23 \mu\text{g}/\text{m}^3$), whereas in coastal PM, it was present at significantly increased levels, ranging between 0.06 and $2.1 \mu\text{g}/\text{m}^3$ (average: $0.49 \mu\text{g}/\text{m}^3$). As far as the seasonal differences are concerned, NH_4^+ reached the maximum levels in the cold season (February/March 2011) for the three studied aerosols fractions over marine sites, similarly to the ammonium-bound secondary aerosols (see above). Likewise, it peaked in the cold season for the coastal, fine and medium-sized aerosols. Interestingly, for the coarse aerosol, sampled at the coastal site, NH_4^+ levels reached the maximum in the late spring, i.e., in May 2011.

The mineral content in the marine fine aerosol was ranging from 0.04 to $0.29 \mu\text{g}/\text{m}^3$ (average: $0.11 \mu\text{g}/\text{m}^3$), whereas in coastal fine aerosol, it showed lower values, and much less fluctuations, i.e., between 0.06 and $0.09 \mu\text{g}/\text{m}^3$ (average: $0.07 \mu\text{g}/\text{m}^3$). The mineral content in medium-sized marine aerosols was a bit higher than in fine aerosol, ranging from 0.08 to $0.33 \mu\text{g}/\text{m}^3$ (mean: $0.21 \mu\text{g}/\text{m}^3$), as well as in the coastal medium-sized aerosol, fluctuating between 0.11 and $0.28 \mu\text{g}/\text{m}^3$ (average: $0.20 \mu\text{g}/\text{m}^3$). In coarse marine PM, the mineral content was observed to be fairly high, as compared to the fine and medium-sized aerosol (range: 0.31– $1.05 \mu\text{g}/\text{m}^3$, average: $0.6 \mu\text{g}/\text{m}^3$), whereas in coastal particulate, it was present at around twice higher levels, ranging between 0.84 and $1.7 \mu\text{g}/\text{m}^3$ (average: $1.2 \mu\text{g}/\text{m}^3$). Interestingly, the mineral content in marine fine aerosols peaked in the cold season (February/March 2011), whereas no clear seasonal tendency could be observed for coastal fine aerosols. The mineral content of medium-sized and coarse marine aerosols developed rather fluctuating average air levels, peaking in the cold season (March 2011). While similar trends could be observed for coastal samples of the same particle size ranges. The BC content in marine PM_{10} was ranging from 0.4 to $1.6 \mu\text{g}/\text{m}^3$ (average: $1.0 \mu\text{g}/\text{m}^3$), and peaked during the cold season (February/March 2011).

The adsorbed water content of marine fine PM was ranging over 0.38– $3.2 \mu\text{g}/\text{m}^3$ (average: $1.04 \mu\text{g}/\text{m}^3$), whereas in coastal fine aerosol, it was present at lower values, fluctuating between 0.29 and $1.21 \mu\text{g}/\text{m}^3$ (average: $0.62 \mu\text{g}/\text{m}^3$). The water content of the medium-sized marine PM was a bit higher than that of the fine aerosol, varying between 0.45 and $1.96 \mu\text{g}/\text{m}^3$ (average: $0.85 \mu\text{g}/\text{m}^3$), as well as in coastal medium-sized aerosol, fluctuating between 0.3 and $2.56 \mu\text{g}/\text{m}^3$ (mean: $0.92 \mu\text{g}/\text{m}^3$). In coarse marine aerosol, the water content was observed to be considerably higher, as compared to the fine and medium-sized aerosol (range: 1.3– $3.0 \mu\text{g}/\text{m}^3$, average: $2.0 \mu\text{g}/\text{m}^3$), as well as in coastal particulate, fluctuating between 0.9 and $2.3 \mu\text{g}/\text{m}^3$ (average: $1.5 \mu\text{g}/\text{m}^3$). It should be mentioned that the estimated concentration of the unaccounted/non-detected aerosol fraction of the fine, medium and coarse marine PM was considerably high, ranging between 2.2 and $6.4 \mu\text{g}/\text{m}^3$ (average: $3.9 \mu\text{g}/\text{m}^3$), between 1.1 and $3.4 \mu\text{g}/\text{m}^3$ (average: $1.9 \mu\text{g}/\text{m}^3$), and between 0.3 and $11.8 \mu\text{g}/\text{m}^3$ (average: $4.8 \mu\text{g}/\text{m}^3$), respectively. Similar, or higher values for the unaccounted fraction of the coastal samples were experienced, ranging between 2.1 and $5.6 \mu\text{g}/\text{m}^3$ (average: $4.1 \mu\text{g}/\text{m}^3$), between 1.4 and $10.6 \mu\text{g}/\text{m}^3$ (average: $4.4 \mu\text{g}/\text{m}^3$), and between 0.6 and $5.9 \mu\text{g}/\text{m}^3$ (average: $2.8 \mu\text{g}/\text{m}^3$), respectively.

3.6. Relative contributions of various species to marine and coastal PM₁₀

The relative contributions of various species detected from marine and coastal aerosols are depicted in Figs. 7 and 8. As can be seen, genuine sea salt contributed with a significant percentage to PM₁₀ mass, and was evidently more abundant in marine samples and the warm season (end of spring, beginning of autumn), e.g., 42% and 22% in May 2010 for marine and coastal areas (Fig. 7). Aged sea salt (bound to NO₃⁻ and SO₄²⁻) contributed about 6–17% to the PM₁₀ mass over the seasons; the weight of SO₄²⁻ bound sea salt was generally about an order of magnitude lower, or even negligible. The contribution was usually a few percent higher, or similar in the coastal samples as compared to the marine aerosols. Ammonium-bound NO₃⁻ and SO₄²⁻ contributed generally with a few percent during the campaigns, except for the early spring (March 2011), when the contribution of the former was 28% and 26% in marine and coastal PM₁₀, respectively. Ammonium contributed generally to a low extent to PM₁₀, ranging from 3 to 12%, with more abundance over the coastal site. Exception was in the early spring (March 2011), when its contribution was as high as 12% for marine PM₁₀, but somewhat lower (9%) values were found in coastal PM₁₀.

The contribution of mineral mass to PM₁₀ was stretching between 2–5% and 3–10% for marine and coastal sites, respectively. For marine samples, more contribution of mineral aerosol was observed during the cold season, whereas for coastal samples, the contribution of mineral content to PM₁₀ was rather lower in winter, e.g., 3–4% in February/March 2011. Black carbon contributed to PM₁₀ mass to a fairly low extent, ranging from 2% to 5%. It showed a rather gradual increase from the late spring aerosols towards those sampled in the cold season (Figs. 7 and 8).

A fairly large amount of adsorbed water was observed in PM₁₀, ranging between 8–18% and 8–13% for marine and coastal samples, respectively, it usually being higher for open sea samples. Moreover, the unaccounted fraction was also high, ranging between 14–45% and

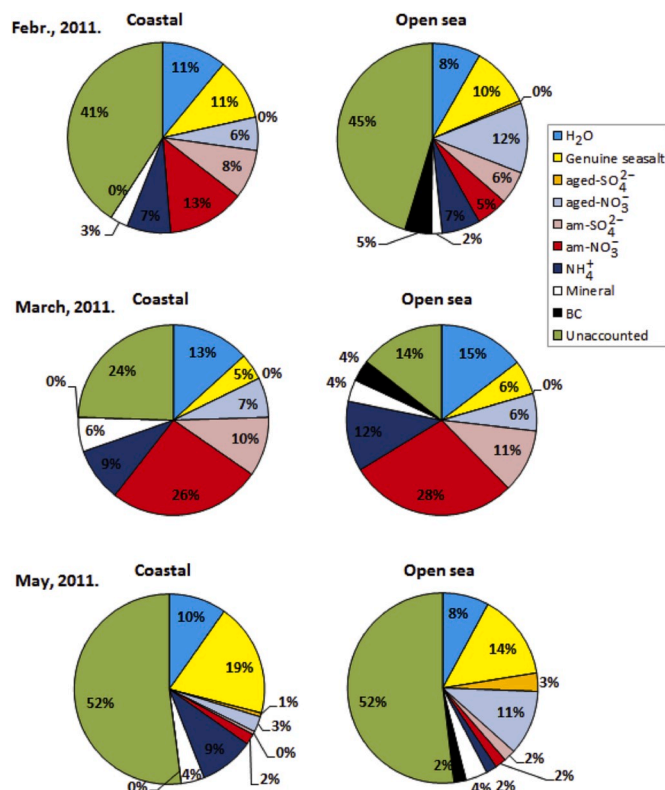


Fig. 8. Distribution of PM₁₀ constituents sampled over open sea areas and the coastal background station of the North Sea in various seasons in 2011.

24–55% for marine and coastal samples, respectively. Obviously, this leaves questions open about the exact chemical composition of these fractions of open sea and coastal aerosols. This necessitates qualitative and quantitative analysis of a much wider set of the particulate components, most probably organic constituents, which research was out of the scope of this study.

3.7. Correlations of weather variables, particulate mass and constituents

Among size-segregated aerosols, the finer fractions, PM₁ and PM_{2.5-1} correlated strongly with each other and the air pressure on the open sea and at the coastal site (Tables S1–S2). The air RH correlated highly with finer PM fractions at the coastal station, while lower correlations were observed for open sea samples. Strong anti-correlations have been recognized for the lower PM fractions with precipitation, while to a lower degree with wind speed, solar radiation, air temperature and sea water temperature. Coarse aerosols (PM_{10-2.5}) correlated strongly with precipitation and somewhat lower with air temperature at the coastal site, whereas they developed anti-correlation with RH. On the open sea, coarse PM correlated loosely with wind speed, air temperature and sea water temperature, and showed no dependence on the other monitored meteorological variables. Overall, the lower PM fractions showed more dependency on weather parameters at the coastal site, as compared to the marine areas.

Bivariate correlation analysis revealed strong correlations of PM₁ and PM_{2.5-1} masses between and within coastal and open sea samples, whereas their loose anti-correlation with the coarse aerosol mass was observed at both kinds of study areas (Table S3). On the other hand, strong correlation was found for coarse PM fractions collected at the coastal station and the open sea. These findings demonstrate the strong coupling between the ambient air pollution of the open sea and the coastal region.

Amongst the ionic components (Tables S4–S5), sea spray related major species, such as Na⁺ and Cl⁻ were correlated rather well with

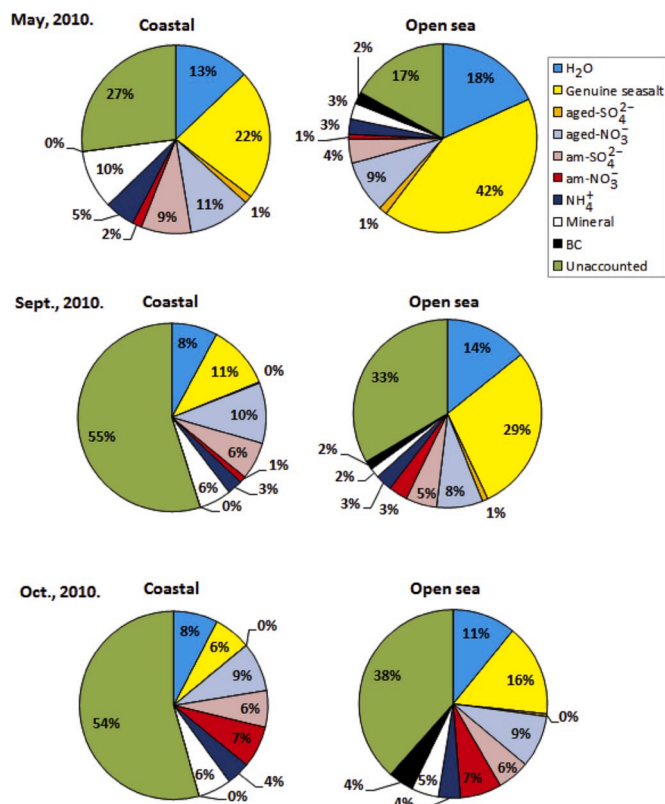


Fig. 7. Distribution of PM₁₀ constituents sampled over open sea areas and the coastal background station of the North Sea in various seasons in 2010.

wind speed and solar radiation in at least two, generally the coarser particulate fractions on the open sea, whilst at the coastal site only coarse Cl^- correlated with them. NH_4^+ was rather strongly anti-correlated with wind speed at the open sea, but loosely correlated with it at the coastal station. Mg^{2+} showed strong correlation with wind speed in $\text{PM}_{10-2.5}$ on the open sea and somewhat lower correlation at the coastal site. Nitrate was anti-correlated with wind speed in each PM fraction, independent of the sampling location, while SO_4^{2-} was anti-correlated with wind speed at least in one of the finer fractions, but correlated with it in coarse PM. Most of the ionic components in the finer PM fractions were anti-correlated with precipitation to a varying degree, whereas coarse Na^+ , K^+ , Mg^{2+} and Cl^- (i.e., major/minor sea spray components) correlated well with it. NH_4^+ correlated fairly well with air pressure and RH in each studied aerosol fraction, independent of the sampling site, but anti-correlated with air temperature, sea water temperature and solar radiation. Fine K^+ correlated with air pressure over open sea areas, and with RH at the coastal site. On the other hand, coarse K^+ correlated with air temperature and sea water temperature over open sea areas. Fine and medium-sized Ca^{2+} strongly correlated with air pressure at coastal and open sea areas, while these components correlated also with RH at the coastal site. Fine and coarse Cl^- correlated well with solar radiation on the open sea. Size-segregated nitrates correlated strongly with air pressure at the open sea and coastal sites, while some dependency on RH was found only at the coastal site for finer PM fractions. Air temperature, sea water temperature and solar radiation developed slight anti-correlation with NO_3^- levels. The other component of secondary inorganic aerosol, sulfate showed similar correlation pattern to that of NO_3^- on the open sea and at coastal station, respectively. Overall, the air levels of ionic species in various size-fractions depended less on seasonal changes in meteorological conditions, existing on the open sea, whereas more influence of these variables could be observed at the coastal station (e.g., wind speed, RH). Looking at the within season correlations of ionic aerosol components between the coastal and open sea samples, strong correlations were recognized, with coefficients ranging between 0.74 and 0.97. This finding is an additional proof of the close relationship of the open sea air pollution with those, observed at the coastal air monitoring station.

3.8. Considerations on yearly/seasonal AIS data and emissions for the Belgian North Sea

The Belgian Continental Shelf belongs to the southern bight of the North Sea, which is the most densely trafficked part of this sea. The yearly individual ship signal data from the automatic identification system (AIS) messages collected and processed for this marine area and the related busy harbors indicate a highly dense traffic throughout the year 2009, as envisaged in a former study (Bencs et al., 2012). In these evaluations, tankers, passenger ships and cargo ships were taken into account, with a total of close to 13.6 million AIS signals (74% of the total AIS messages). The high density of ship traffic in general does not significantly change over the seasons regarding the message frequencies received from the national and international routes of the Belgian North Sea. This is manifested in the received seasonally similar amounts of AIS signal data by Belgian marine and coastal AIS stations in 2009. The NO_x and SO_2 emissions observed for the region on the basis of AIS signals and individual ship emission data were in good agreement with those observed from predictive data of the MOPSEA model for 2010. Moreover, this finding is supported by a more recent research, conducted in 2016 for ship activities on the North Sea, assessed on the basis of the AIS signals of ships by Nilsson et al. (2018). This research team concluded a slightly higher density of ship traffic over the southern North Sea for the summer season, as compared to the other seasons. This and the current findings are strong indicators that the seasonal variation in ship traffic density has low influence on air pollution at coastal and open waters, as well as coastal areas of the southern North Sea, but most likely the seasonal periodicity of the weather and the extent of emissions by ships

play a vital role.

4. Conclusions

In this research, the southern bight of the North Sea at Belgium and the English Channel was studied from the viewpoint of seasonality of ship emission related atmospheric pollution, i.e., atmospheric gases, size-segregated aerosols and their elemental and ionic constituents and the black carbon content. The results observed for marine areas were compared to those obtained from a coastal background station at De Haan, Belgium. For coarse aerosol ($\text{PM}_{10-2.5}$) and PM_{10} mass of marine origin, a rather increasing trend of aerosol mass could be observed from late spring, peaking in winter. The medium-sized ($\text{PM}_{2.5-1}$) and the fine (PM_1) marine aerosols followed a similar trend; each developed a concentration growth in the cold season. The concentrations of gaseous air pollutants (e.g., HNO_2 , HNO_3 , HCl , SO_2 , NH_3) originating from exhaust fumes of ocean-going ships were mostly peaking in the cold season as well.

The mostly crustal/upper soil related (mineral) aerosol components were more apparent in the coarse PM and especially during winter with increased airborne levels. Although these elements were present at low amounts in fine PM, some seasonality could be observed with their enhanced air levels in the cold season. This is likely indicative of the release of higher amounts of these elements into the ambient air, due to increased heavy oil combustion, for instance, in terms of larger ship emissions, as well as increased air levels over the coastal monitoring station. This assumption is also supported by results for anthropogenic trace metals of heavy oil burning (such as Ni, V, Cu, Mn, Pb), found to be present at increased amounts in marine and coastal fine aerosols.

The concentration trends of total (inorganic) ionic species sampled over the sea and at the coastal station were usually similar to that of the corresponding PM masses, i.e., the increasing levels from late spring towards the cold season, when reaching peak values. Sea salt bound fine sulfate and nitrate peaked in spring or the cold season for marine areas, whereas for the coastal site they reached the maximum in the cold season. The components of secondary inorganic aerosols (ammonium nitrates and sulfates) peaked in the cold season for all the three studied aerosols fractions over marine sites, while similar seasonal trends could be observed for the coastal station.

The observed general tendency of aerosol distribution over the study areas is independent of the sampling site: the higher the aerosol mass on the open sea with ship traffic, the higher the suspended particulate mass sampled at the coast. This finding is an addition and firm proof that the marine pollution sources such as national and international shipping have a direct effect on coastal air quality, and most likely the health of the population living nearby areas.

Declaration of Competing Interest

The authors declare that they have no known competing financial interests or personal relationships that could have appeared to influence the work reported in this paper.

CRediT authorship contribution statement

László Bencs: Conceptualization, Investigation, Methodology, Validation, Supervision, Data curation, Writing - original draft, Writing - review & editing. **Benjamin Horemans:** Conceptualization, Investigation, Methodology, Validation, Data curation, Writing - review & editing. **Anna Jolanta Buczyńska:** Conceptualization, Investigation, Methodology, Validation, Writing - review & editing. **Felix Deutsch:** Conceptualization, Investigation, Methodology, Resources, Supervision, Writing - review & editing. **Bart Degraeuwe:** Conceptualization, Methodology, Investigation, Resources, Writing - review & editing. **Martine Van Poppel:** Investigation, Methodology, Resources, Writing - review & editing. **René Van Grieken:** Conceptualization, Methodology,

Investigation, Resources, Supervision, Funding acquisition, Project administration, Writing - review & editing.

Acknowledgments

The participating researchers of this study gratefully acknowledge the funding from the Belgian Science Policy Office (BELSPO) under the SHIPFLUX project (assignment No.: SD/NS/07A). The researchers thank Jan Van Loock (UA), André Cattrijsse (VLIZ) and Frank Broucke (VLIZ) for their help with the logistics, sampling and organization of the field/marine studies and Francisco (Tjess) Hernandez (VLIZ) for his help in getting access to the weather data. The participants also want to express their sincere thanks to the crew of R/V Belgica for their help and cooperation in the marine expeditions.

Appendix A. Supplementary data

Supplementary data to this article can be found online at <https://doi.org/10.1016/j.aeoa.2020.100077>.

References

- Alver, F., Saraç, B.A., Şahin, Ü.A., 2018. Estimating of shipping emissions in the samsun port from 2010 to 2015. *Atmos. Pollut. Res.* 9, 822–828.
- Agrawal, H., Malloy, Q.G.J., Welch, W.A., Miller, J.W., Cocker, D.R., 2008. In-use gaseous and particulate matter emissions from a modern ocean going container vessel. *Atmos. Environ.* 42, 5504–5510.
- Alföldy, B., Balzani Lööv, J., Lagler, F., Mellqvist, J., Berg, N., Jörg Beecken, J., Weststrate, H., Duyzer, J., Bencs, L., Benjamin Horemans, B., Cavalli, F., Putaud, J. Ph, Janssens-Maenhout, G., Pintér Csordás, A., Van Grieken, R., Borowiak, A., Hjorth, J., 2013. Measurements of air pollution emission factors for marine transportation in SECA. *Atmos. Meas. Tech.* 6, 1777–1791.
- Anaf, W., Horemans, B., Van Grieken, R., De Wael, K., 2012. Chemical boundary conditions for classification of aerosol particles using computer controlled electron probe microanalysis. *Talanta* 101, 420–427.
- Anaf, W., Horemans, B., Madeira, T.I., Carvalho, M.L., De Wael, K., Van Grieken, R., 2013. Effects of a constructional intervention on airborne and deposited particulate matter in the Portuguese National Tile Museum, Lisbon. *Environ. Sci. Pollut. Res.* 20, 1849–1857.
- Åström, S., Yaramenka, K., Winnes, H., Fridell, E., Holland, M., 2018. The costs and benefits of a nitrogen emission control area in the Baltic and North Seas. *Transport. Res. Part D* 59, 223–236.
- Bencs, L., Horemans, B., Buczyńska, A.J., Van Grieken, R., Viaene, P., Veldeman, N., Deutsch, F., Degraeuwe, B., Van Poppel, M., Lauwaet, D., De Ridder, K., Janssen, L., Maiheu, B., Vanhulsel, M., Janssen, S., Blyth, L., Mensink, C., 2012. Atmospheric deposition fluxes to the Belgian marine waters originating from ship emissions. “SHIPFLUX” project (Final Report) Belspo Program, Science for a Sustainable Development (SSD). Website. http://www.belspo.be/belspo/SSD/science/Reports/SHIPFLUX_FinRep_AD.pdf. accessed: April 28th, 2020.
- Bencs, L., Horemans, B., Buczyńska, A.J., Van Grieken, R., 2017. Uneven distribution of inorganic pollutants in marine air originating from ocean-going ships. *Environ. Pollut.* 222, 226–233.
- Blasco, J., Durán-Grados, V., Hampel, M., Moreno-Gutiérrez, J., 2014. Towards an integrated environmental risk assessment of emissions from ships' propulsion systems. *Environ. Int.* 66, 44–47.
- Chen, G., Huey, L.G., Trainer, M., Nicks, D., Corbett, J., Ryeson, T., Parrish, D., Neuman, J.A., Nowak, J., Tanner, D., Holloway, J., Brock, C., Crawford, J., Olson, J. R., Sullivan, A., Weber, R., Schaffner, S., Donnelly, S., Atlas, E., Roberts, J., Flocke, F., Hübler, G., Fehsenfeld, F., 2005. An investigation of the chemistry of ship emission plumes during ITCT 2002. *J. Geophys. Res.* 110 (D10S90), 1–15.
- Chu-Van, T., Ristovski, Z., Pourkhesalian, A.M., Rainey, T., Garaniya, V., Abbassi, R., Jahangiri, S., Enshaei, H., Kam, U.S., Kimball, R., Yang, L., Zare, A., Bartlett, H., Brown, R.J., 2018. On-board measurements of particle and gaseous emissions from a large cargo vessel at different operating conditions. *Environ. Pollut.* 237, 832–841.
- Cooper, D.A., Peterson, K., Simpson, D., 1996. Hydrocarbon, PAH and PCB emissions from ferries: a case study in the Skagerak – kattegat – Öresund region. *Atmos. Environ.* 30, 2463–2473.
- Cooper, D.A., 2001. Exhaust emissions from high speed passenger ferries. *Atmos. Environ.* 35, 4189–4200.
- Cooper, D.A., 2003. Exhaust emissions from ships at berth. *Atmos. Environ.* 37, 3817–3830.
- Corbett, J.J., Winebrake, J.J., Green, E.H., Kasibhatla, P., Eyring, V., Lauer, A., 2007. Mortality from ship emissions: a global assessment. *Environ. Sci. Technol.* 41, 8512–8518.
- De Meyer, P., Maes, F., Volckaert, A., 2008. Emissions from international shipping in the Belgian part of the North Sea and the Belgian seaports. *Atmos. Environ.* 42, 196–206.
- Dalsøren, S.B., Eide, M.S., Endresen, Ø., Mjelde, A., Gravir, G., Isaksen, I.S.A., 2009. Update on emissions and environmental impacts from the international fleet of ships: the contribution from major ship types and ports. *Atmos. Chem. Phys.* 9, 2171–2194.
- Davis, D.D., Grodzinsky, G., Kasibhatla, P., Crawford, J., Chen, G., Liu, S., Bandy, A., Thornton, D., Guan, H., Sandholm, S., 2001. Impact of ship emissions on marine boundary layer NO_x and SO₂ distributions over the Pacific Basin. *Geophys. Res. Lett.* 28, 235–238.
- de la Rosa, J.D., Sánchez de la Campa, A.M., Alastuey, A., Querol, X., González-Castanedo, Y., Fernández-Camacho, R., Stein, A.F., 2010. Using PM₁₀ geochemical maps for defining the origin of atmospheric pollution in Andalusia (Southern Spain). *Atmos. Environ.* 44, 4595–4605.
- Eyring, V., Isaksen, I.S.A., Bernsten, T., Collins, W.J., Corbett, J.J., Endresen, Ø., Grainger, R.G., Moldanova, J., Schlager, H., Stevenson, D.S., 2010. Transport impacts on atmosphere and climate: shipping. *Atmos. Environ.* 44, 4735–4771.
- Horemans, B., Krata, A., Buczyńska, A.J., Dirtsu, A.C., Van Meel, K., Van Grieken, R., Bencs, L., 2009. Major ionic species in size-segregated aerosols and associated gaseous pollutants at a coastal site on the Belgian North Sea. *J. Environ. Monit.* 11, 670–677.
- IMPROVE (Interagency Monitoring of Protected Visual Environments), 2020. Website. <http://vista.cira.colostate.edu/improve/tools/aerotypeqs.htm>. accessed: April 29th.
- Kreidenweis, S.M., Petters, M.D., DeMott, P.J., 2008. Single-parameter estimates of aerosol water content. *Environ. Res. Lett.* 3 (7), 035002.
- Lack, D.A., Corbett, J.J., Onasch, T., Lerner, B., Massoli, P., Quinn, P.K., Bates, T.S., Covert, D.S., Coffman, D., Sierau, B., Herndon, S., Allan, J., Baynard, T., Lovejoy, E., Ravishankara, A.R., Williams, E., 2009. Particulate emissions from commercial shipping: chemical, physical, and optical properties. *J. Geophys. Res.: Atmos.* 114, D00F04.
- Li, J., Chen, B., Sánchez de la Campa, A.M., Alastuey, A., Querol, X., de la Rosa, J.D., 2018. 2005–2014 trends of PM₁₀ source contributions in an industrialized area of southern Spain. *Environ. Pollut.* 236, 570–579.
- Liu, H., Jin, X., Wu, L., Wang, X., Fu, M., Lv, Z., Morawska, L., Huang, F., He, K., 2018. The impact of marine shipping and its DECA control on air quality in the Pearl River Delta, China. *Sci. Total Environ.* 625, 1476–1485.
- Maenhaut, W., Cafmeyer, J., Dubtsov, S., Chi, X., 2002. Detailed mass size distribution of elements and species, and aerosol chemical mass closure during fall 1999 at Gent, Belgium. *Nucl. Instrum. Methods Phys. Res. B* 189, 238–242.
- Moldanova, J., Fridell, E., Popovicheva, O., Demirdjian, B., Tishkova, V., Faccineto, A., Focsa, C., 2009. Characterisation of particulate matter and gaseous emissions from a large ship diesel engine. *Atmos. Environ.* 43, 2632–2641.
- Mölders, N., Porter, S.E., Cahill, C.F., Grell, G.A., 2010. Influence of ship emissions on air quality and input of contaminants in southern Alaska National Parks and Wilderness Areas during the 2006 tourist season. *Atmos. Environ.* 44, 1400–1413.
- MUMM – Management Unit of Mathematical Models of the North Sea, 2020. website. <http://odnature.naturalsciences.be/belgica/en/odas>. accessed: April 27th.
- Murena, F., Mocerino, L., Quaranta, F., Toscano, D., 2018. Impact on air quality of cruise ship emissions in Naples, Italy. *Atmos. Environ.* 187, 70–83.
- MVB (Meetnet Vlaamse Banken – Monitoring Network of the Flemish Banks), 2020. website. <https://meetnetvlaamsebanken.be/>. last accessed: April 29th, 2020.
- Nilsson, H., van Overloop, J., Mehdi, R.A., Pålsson, J., 2018. Transnational maritime spatial planning in the North sea: the shipping context. Report on Work-package 4 of the NorthSEE Project. Interreg VB North Sea Region. www.northsearegion.eu/media/4836/northsee_finalshippingreport.pdf. accessed: April 29th, 2020.
- Pandolfi, M., González-Castanedo, Y., Alastuey, A., de la Rosa, J.D., Mantilla, E., de la Campa, A.S., Querol, X., Pey, J., Amato, F., Moreno, T., 2011. Source apportionment of PM₁₀ and PM_{2.5} at multiple sites in the strait of Gibraltar by PMF: impact of shipping emissions. *Environ. Sci. Pollut. Res.* 18, 260–269.
- Poplawski, K., Setton, E., McEwan, B., Hrebenyuk, D., Graham, M., Keller, P., 2011. Impact of cruise ship emissions in Victoria, BC, Canada. *Atmos. Environ.* 45, 824–833.
- Popovicheva, O., Kireeva, E., Persiantseva, N., Timofeev, M., Bladt, H., Ivleva, N.P., Niessner, R., Moldanova, J., 2012. Microscopic characterization of individual particles from multicomponent ship exhaust. *J. Environ. Monit.* 14, 3101–3110.
- Querol, X., Viana, M., Alastuey, A., Amato, F., Moreno, T., Castillo, S., Pey, J., de la Rosa, J., Sánchez de la Campa, A., Artíñano, B., Salvador, P., García Dos Santos, S., Fernández-Patier, R., Moreno-Grau, S., Negral, L., Mingüillón, M.C., Monfort, E., Gil, J.I., Inza, A., Ortega, L.A., Santamaría, J.M., Zabalza, J., 2007. Source origin of trace elements in PM from regional background, urban and industrial sites of Spain. *Atmos. Environ.* 41, 7219–7231.
- Tao, J., Zhang, L., Cao, J., Zhong, L., Chen, D., Yang, Y., Chen, D., Chen, L., Zhang, Z., Wu, Y., Xia, Y., Ye, S., Zhang, R., 2017. Source apportionment of PM_{2.5} at urban and suburban areas of the Pearl River Delta region, south China - with emphasis on ship emissions. *Sci. Total Environ.* 574, 1559–1570.
- Van Meel, K., Horemans, B., Krata, A., Bencs, L., Buczyńska, A.J., Dirtsu, A.C., Worobiec, A., Van Grieken, R., 2010. Elemental concentrations in aerosols at the Belgian coast versus seasons and air mass trajectories. *Environ. Chem. Lett.* 8, 157–163.
- Viana, M., Amato, F., Alastuey, A., Querol, X., Moreno, T., García Dos Santos, S., Herce, M.D., Fernández-Patier, R., 2009. Chemical tracers of particulate emissions from commercial shipping. *Environ. Sci. Technol.* 43, 7472–7477.
- Wang, W., Yu, J., Cui, Y., He, J., Xue, P., Cao, W., Ying, H., Gao, W., Yan, Y., Hu, B., Xin, J., Wang, L., Liu, Z., Sun, Y., Ji, D., Wang, Y., 2018. Characteristics of fine particulate matter and its sources in an industrialized coastal city, Ningbo, Yangtze River Delta, China. *Atmos. Res.* 203, 105–117.
- Xu, L., Jiao, L., Hong, Z., Zhang, Y., Du, W., Wu, X., Chen, Y., Deng, J., Hong, Y., Chen, J., 2018. Source identification of PM_{2.5} at a port and an adjacent urban site in a coastal city of China: impact of ship emissions and port activities. *Sci. Total Environ.* 634, 1205–1213.
- Zelenyuk, A., Cai, Y., Chieffo, L., Imre, D., 2005. High precision density measurements of single particles: the density of metastable phases. *Aerosol Sci. Technol.* 39, 972–968.